Functional tests of an *in vitro* maintenance system prototype type organ-on-chip for skeletal muscle

Diana S. Ruvalcaba Martínez,
Christian Chapa González,
Eduardo I. Acosta Gómez and
Esmeralda S. Zuñiga Aguilar*

Electrical and Computing Engineering Department,
Universidad Autónoma de Ciudad Juárez,
Cd. Juárez Chih., CP 32310, México
Email: al141220@alumnos.uacj.mx
Email: christian.chapa@uacj.mx
Email: eduardo.acosta@uacj.mx
Email: esmeralda.zuniga@uacj.mx
*Corresponding author

Abstract: Due to the necessity to develop new systems which maintains the proper conditions for cell growth and cell interaction *in vitro* this work has focused on the characterisation of two models of maintenance system prototypes type organ-on-chip skeletal muscle tissue of neonatal mouse. Cell growth were monitored four days. The images of the cells were obtained through an optical microscope to measure the variations of the alignment angle, the analysis was performed using the ImageJ software. It is concluded that the two OoC prototype models delimit and help cell alignment, but because the surface of the microchannels was not homogeneous or completely flat, adding to this the depth factor, the cell proliferation was affected. As a result, we demonstrated that the proposed organ-on-chip system promotes cell alignment.

Keywords: organ-on-chip; OoC; cell alignment; microchannels.

Reference to this paper should be made as follows: Ruvalcaba Martínez, D.S., Chapa González, C., Acosta Gómez, E.I. and Zuñiga Aguilar, E.S. (xxxx) 'Functional tests of an *in vitro* maintenance system prototype type organ-on-chip for skeletal muscle', *Int. J. Biomedical Nanoscience and Nanotechnology*, Vol. X, No. Y, pp.xxx–xxx.

Biographical notes: Diana S. Ruvalcaba Martínez was a student in the Universidad Autónoma de Ciudad Juárez of Biomedical Engineering program. She was working with the Biopolymers and Bioprinting Lab of the same university.

Christian Chapa González is a Research Professor at the Institute of Engineering and Technology of the Universidad Autónoma de Ciudad Juárez, and the Head of the NANOMEDICINA-UACJ research group. His research interest focuses on nanomedicine, biomaterials and bioprinting, where theragnostic approach is the main goal. He received his PhD in Materials Science in 2014.

Eduardo I. Acosta Gómez is a Research Professor at the Universidad Autónoma de Ciudad Juarez and in the Pharmacology Laboratory of the same university. His research interests include pharmacology, physiology, and functional genetics.

Esmeralda S. Zuñiga Aguilar is a Research Professor at the Universidad Autónoma de Ciudad Juarez. She is currently working in collaboration with the Biopolymers and Bioprinting Lab of the same university. Her areas of interest are focused on tissue engineering, new generation materials and *in vitro* maintenance systems. She obtained her Doctor of Science in Biomedical Engineering in 2014 from the Universidad Autónoma Metropolitana.

1 Introduction

The skeletal muscle is formed by muscle bundles and in turn these are composed by muscular fibres. Also, the skeletal muscle is composed by conjunctive tissue layers, the endomysium surrounds the muscular fibres, the perimysium groups the muscle fibres into bundles of muscle fibres, the epimysium covers the entire muscle. After the epimysium, there is a fine network of capillaries which guaranteed muscle vascularity. Muscle cells are organised into fascicles and are joined by connective tissue. Muscle fibre or myocyte is the functional unit of skeletal muscle, it is elongated and the union of these make up the muscle bundle (AFM and ASEM, 2003). Additionally, the muscle fibre is surrounded by the sarcolemma, which is the cytoplasm of the muscle fibre. It contains the endoplasmic reticulum, mitochondria, reticulin fibres and glycoproteins (endomysium), bands I and A, longitudinal and transversal striations, and zone Z (Zuñiga Aguilar, 2014). The striations of myofibril are composed by myofilaments, there are two types the thick myofilament composed of myosin and the thin myofilament composed of action (AFM and ASEM, 2003), this is an important factor for the cell alignment. For a better understanding of this muscle, culture techniques have been used, in the past researchers had two options: *in vitro* cultures of human cells and animal models, but in both were problems such as the extraction of primary cells, altered phenotypes, to name a few (Sakolish et al., 2016).

The technology in cultivation techniques has a great development, so the technologies have decreased in size. In 2011, the ‘human on chip’ project was announced and currently biomimetic systems consisting of microfluidic chips developed with microtechnology, called organ on a chip, have managed to mimic the main functions of human organs, with some limitations (Sun et al., 2016). The emergence of these devices arises to circumvent serious limitations of *in vitro* and *in vivo* cultures, since they are unable to predict, on their own, responses of complex organisms or tissues such as the response to drugs, external mechanical, biochemical or physicochemical stimuli. Researchers are currently looking at the organ-on-chip (OoC) to reproduce the organ’s physiological conditions to overcome these limitations.

OoC approaches are quite varied. One of the most popular OoC approaches is to study cancer metastasis, also called chip metastasis. In it, researchers study cell propagation and cytokinesis (Caballero et al., 2017). Another interesting field is Kidney on chip, in which a part of tissue from the proximal tubules of the kidney is used to detect biomarkers in order to predict drug interactions (Wilmer et al., 2016). OoC research has

intensified in recent years, encompassing organs such as the heart and lungs, as well as microvascular networks and blood-brain barriers. Such OoC approaches seek to predict the body's pharmacological responses, as well as organ physiology and pathology (Halldorsson et al., 2015). However, there is not a great variety of research regarding OoC focused on skeletal muscle, this is important since it is the most abundant tissue and the largest organ in the locomotor and metabolic system of the human body, which requires a more advanced understanding of its structure, composition and function (Jena et al., 2019). *In vitro* cultures are manageable, lower cost and accessible but do not achieve the reproduction of cell-cell and cell-ECM (extra cellular matrix) interactions, apart from lack of vascularity and the lack of pharmacological metabolism process reproduction. Due to these deficiencies in *in vitro* cultures, animal models are used (Sakolish et al., 2016). Animal models are genetically like humans, have a moderate pharmacokinetic prediction, however they are high cost, not human predictive, and fail to reproduce specific characteristics of the human body such as the immune system, stem cell differentiation, to name a few. Aside from ethical issues involved in their practice (Caballero et al., 2017). Consequently, this research seeks to solve the problem that *in vitro* cultures and animal models fails to reproduce, as cellular processes, interactions, and a better representation of the morphology of the functional unit of skeletal muscle tissue in the human body (Materne et al., 2015).

2 Methodology

This work seeks the functional characterisation of an OoC capable of biomimeticing the functions or morphological characteristics of a myofibril of skeletal muscle tissue, this device seeks to maintain adequate conditions for cell growth and cell interaction. The morphology, degree of alignment of cells in microchannels and cell viability in the OoC will be studied, using functional tests of the prototype for its verification. In addition, two types of *in vitro* maintenance will be compared, one using conventional culture dishes, and the other using OoC prototype models evaluating the viability of each. The research was composed of mouse neonatal skeletal muscle removal, cell dissociation, myoblast and fibroblast separation to cell seeding in culture dishes and in prototypes. The methodology was based on functional tests to a 35 mm culture dish and an n = 3, to evaluate the prototypes of two types of model: the PDMS channel model (Dow Corning Sylgard 184) in 35 mm culture dishes and the OoC model of PDMS on slides.

2.1 Skeletal muscle cells from mouse neonates obtention

For skeletal muscle cells obtention, four CD4 new-born mice of 3–5 days old were used, which were sacrificed by carbon dioxide inhalation. The upper and lower limbs of the mouse neonates were cleaned with 70% ethanol, the skin was removed using microdissection forceps, and the four members of the trunk of the mouse neonates were cut with surgical stainless-steel curved tip scissors. To separate the muscle from the bone from each limb microdissection forceps were used, this was do it with a visual support of a VELAB stereoscopic microscope mod. VE-S6 at 40x magnification. The tissue obtained from the dissection was placed in a Petri dish on ice, which was covered with PBS (GIBCO). The disintegration procedure started with the mechanical disintegration of the tissue by means of the microdissection forceps, then the enzymatic disintegration of

the tissue was started, performed by an enzymatic solution composed of 2 ml of Collagenase D (Roche) [1.5 U/ml], 2 ml of Dispase II (Sigma Aldrich) [2.4 U/ml] and 100 µl $CaCl_2$ (Sigma Aldrich) [2.5 mM], see Figure 1. The new-born mice were managed under the norm NOM-062-ZOO-1999 and with the approval of the institutional committee of ethics and bioethics of the Universidad Autonoma de Ciudad Juarez, CIEB-2019-1-038.

Figure 1 Primary cell culture obtention (see online version for colours)

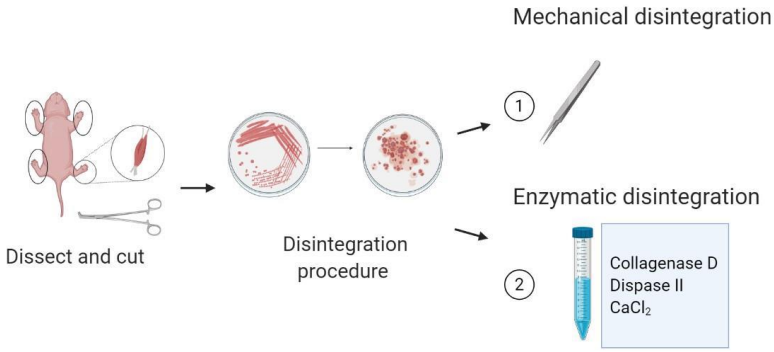

The Petri dish with the disaggregated tissue was placed in the CO_2 incubator for 15 minutes, then the mechanical disaggregation was continued, this procedure (incubator-mechanical disaggregation) was repeated five times. Then it was filtered through an 80 µm diameter filter (SIGMA) to remove any remaining large pieces of tissue, in which were added 10 ml of pre-seeding culture medium supplemented with 90% Ham's F-10 (GIBCO), 10% Newborn Calf Serum (NBCS, GIBCO) and 1% anti-anti (GIBCO). The solution was transferred from the Petri dish to a 15 ml Falcon tube and then centrifuged for 5 minutes at 1,400 rpm.

Consequently, the supernatant was removed and the cells were pre-seeded with pre-seeded culture medium that was placed inside the incubator for 20 minutes. This resulted that non-adherent cells were removed by carefully moving the Petri dish circularly and rinsing with 1 ml of pre-seeding culture medium.

2.2 Culture and differentiation of muscle cells

The culture was transferred from the Petri dish to 15 ml Falcon tubes and centrifuged for 5 minutes at 1,400 rpm. The supernatant was removed to then add the primary myoblast growth medium (F-10, GIBCO) supplemented with 80% Ham's F-10 (GIBCO), 20% NBCS (GIBCO), and 1% antibiotic-antifungal (GIBCO). The culture was placed in 60 mm culture dishes with 10 ml of medium. Growth conditions (5.0% CO_2 at 37.2°C) were maintained for the cells. The medium was changed every two days; for the last fibroblast clearance the cells were subculture for at least 30 days. Myoblast growth medium (F-10, GIBCO) was exchanged for myoblast enriched medium due to fibroblasts decrease and myoblasts increase in the cell population. Therefore, a cell fusion was carried out for the formation of myofibrils in the culture due to the exchange of myoblast enriched medium for the Fusion medium.

2.3 Skeletal muscle cells seeding

When the elimination of fibroblasts was achieved, cell seeding was performed in 35 mm culture dishes, which served as a control (Figure 2). The OoC prototypes for the first model used for skeletal muscle were designed and manufactured from PDMS in 35 mm culture dishes, where the emptying guides made by 3D printing were placed, the guides served to shape the growth microchannels and delimit the emptying of PDMS (Figure 3). The other OoC model was made using the PDMS casting technique on slides, in monocure photocurable resin moulds printed by the 3D printing technique (Figure 4), the two OoC models were made considered seeding microchannels to limit and guide cell growth in a certain area as well as direct cell alignment. Seeding was carried out in the PDMS channels, where the cells were maintained with a myoblast enriched culture medium. The culture medium was changed by fusion medium, which was supplemented by 95% D-MEM, 5% inactivated horse serum (HS, GIBCO) and 1% antibiotic-antifungal, to achieve fusion of myoblast aggregations.

2.3.1 Culture dishes seeding

When cell culture was differentiated and forming tissue with an optimal cell growth, trypsinisation was performed, the process was carried out by adding 1 ml of trypsin (0.25% + EDTA, 1 mM, in PBSA) to the culture. After that, incubation for five minutes was performed, then the tip of the micropipettes was washed to begin detaching the cells from the bottom. Subsequently, 2 ml of fusion medium was added, after adding the fusion medium, 1.5 ml were added to two 35 mm culture dishes. Where one was used as a control, see procedure in Figure 2.

Figure 2 Representation of seeding in culture dishes 35 mm, image made in bio render (see online version for colours)

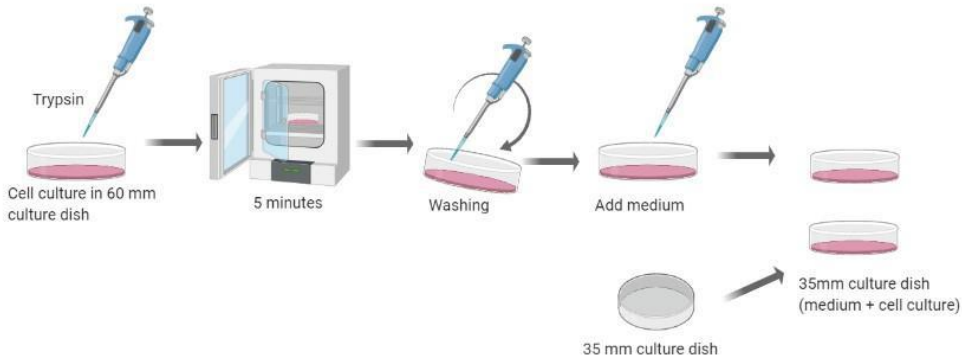

2.3.2 Model of PDMS channels in 35 mm culture dishes seeding

The model of PDMS channels in 35 mm culture dishes (n = 3) (Figure 3), was kept one day before under UV light for 6 hours to dry the PDMS prototype. The next day, a 35 mm culture dish was trypsinised so the cells could detach from the bottom of the culture

dish and then be able to carry out the seeding in the channels of the model. 100 µl of the culture dish were added to each channel, then the prototype was left in the incubator for 4 hours to prevent the evaporation of cell culture and allow the cells to anchor in the three channels of the model, as observed in Figure 3, delimiting the seeding area. After 4 hours of incubation, 1 ml of medium was added, this medium was changed every day for five days.

Figure 3 Representation of seeding on model of PDMS channels in 35 mm culture dishes, image made in bio render (see online version for colours)

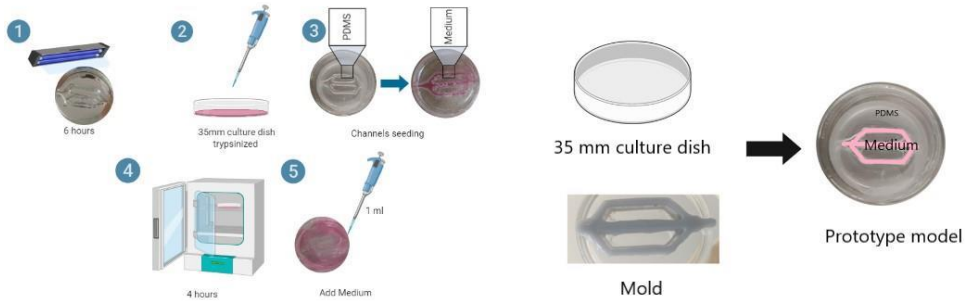

2.3.3 Model of PDMS OoC on slides seeding

The procedure of seeding in the model of PDMS OoC on slides (n = 3) was as follows, see Figure 4, The model was kept one day before under UV light for 6 hours. On the following day was performed a pig skin gelatine treatment for coating (0.1%), the prototype was left to incubate for 24 hours. The next day, was washed with PBS (GIBCO). Subsequently, a 35 mm culture dish was trypsinised so the cells can be detached from the bottom of the culture dish and be able to carry out the seeding in the PDMS channels of the prototype. The seeding was carried out between the PDMS channels, where 100 µl of the culture plate already trypsinised was added to each channel of the prototype, then it was left in the incubator for 4 hours to prevent cell culture from evaporating and allowing cells anchor in the three channels of the model, as seen in Figure 4, delimiting the seeding area. After 4 hours, 1 ml of fusion medium was added, and it was changed every 24 hours for five days.

Figure 4 Representation of seeding on model of PDMS OoC on slides, image made in bio render (see online version for colours)

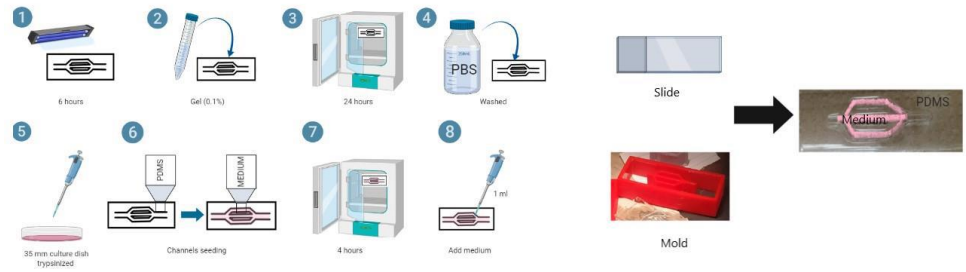

2.4 Model of PDMS OoC on slides seeding

The seeding was performed in culture plates and in two OoC models:

1 model of PDMS channels in 35 mm culture dishes

2 model of PDMS OoC on slides.

PDMS channels were performed to promote cell alignment and its controlled and directed growth. Myoblast-enriched culture medium was added to increase proliferation and then changed to fusion medium, where the cells were kept for five days.

2.5 High resolution images obtention

The scanning electron microscope (SEM) (Hitachi, Mod. SU5000) was used to obtain a description of the microchannels morphology with high resolution images. The microchannels were dried to be observed in the SEM, conductive carbon tape was used to fix the material. Finally, the sample was observed under the SEM.

2.6 Nuclear staining with Hoechst

Hoechst is a cellular permeable fluorescent component that can stain the DNA of eukaryotic and prokaryotic cells. When Hoechst binds to DNA and is excited by ultraviolet light, blue fluorescence is emitted and can be detected with the microscope. An advantage of the Hoechst is its permeability to the membrane, to stain living cells since it binds to DNA regions rich in adenine-thymine in the minor sulcus. When bound to DNA, the fluorescence increases (Crowley et al., 2016). For this reagent characteristic, it is used for nuclear staining, the procedure was as following: the prototype was washed twice with PBS (GIBCO), then 1 ml of PBS (GIBCO) was prepared with 5 µl of Hoechst 333342 (Sigma-Aldrich) and poured into the microchannels of the prototype OoC models. It was placed 30 minutes in the incubator. Subsequently, it was washed with PBS (GIBCO) twice to observe nuclear staining in living cells with ultraviolet light under a microscope. The procedure was performed in a dark room.

3 Results and analysis

To study the consequences of the cell environment on cell viability and cell alignment, the cell culture was seeded in a culture dish, three prototypes of the PDMS channels in 35 mm culture dishes model and three prototypes of the PDMS OoC on slides model as seen in Figure 5.

3.1 Cell culture growth in culture dishes

In the first stage of cell culture maintenance, cell growth was monitored in culture dishes, images captured by stereoscopic microscope (VELAB, Mod. VE-S6) were obtained every three days until reaching 15 days, see Figure 6.

Figure 5 Cell seeding results, (a) culture dishes seeding (b) PDMS channels in 35 mm culture dishes model seeding (c) PDMS OoC on slides model seeding (see online version for colours)

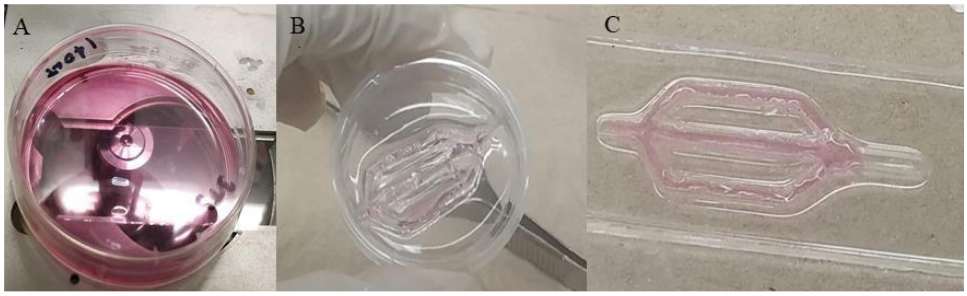

Figure 6 Cell culture growth in culture dishes, (a) taken on 10 September 2019 (b) taken on 13 September 2019 (c) taken on 17 September 2019 (d) taken on 20 September 2019

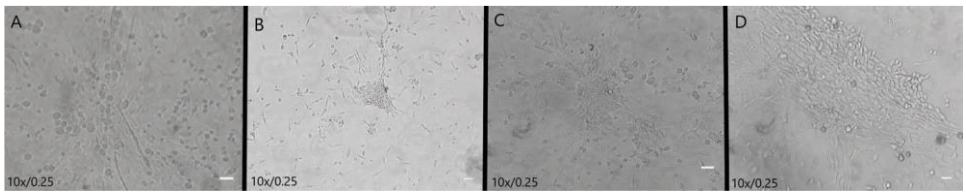

Notes: Phase contrast, scale bar = 500 micron, amplification x250.

In Figure 6(a), a greater growth of myocytes could be observed, although there is still a population of fibroblasts. In Figures 6(b) and 6(c) myoblast fusion began to be observed to begin to form tissue, and a larger population of myoblasts was observed. In Figure 6(d) the myoblasts created an alignment to begin to form myofibrils to create the tissue.

3.2 Skeletal muscle cells seeding

To study cellular behaviour in 2D *in vitro* models, images were taken every 24 hours for five days by the conventional brightfield microscope (ZEISS, Mod. Axio Vert. A1), see Figure 7.

In Figure 7(a) a low myocyte population is observed, because is day 1 a non-adherent cluster of myocytes is observed, that is, suspended in the medium. In Figure 7(b) it is observed that on day 2 there is an increase in the cell population and an anchorage in the substrate begins to be observed. In Figure 7(c), on the third day an increase in the number of anchored cells is observed. In Figure 7(d) on the fourth day of cell culture cell proliferation is increasing. To check the cellular behaviour in the microenvironment created in the OoC microchannels, a control was performed taken images every day during five days of incubation of the six prototypes, three prototypes of the model of PDMS channels in 35 mm culture dishes, see Figure 8, and three prototypes of the model of PDMS OoC on slides, see Figure 9.

Figure 7 Results of images taken by conventional brightfield microscope, (a) (b) (c) (d) skeletal muscle myocytes from mouse neonates in 35 mm culture dishes, images from days 1 to 4, respectively

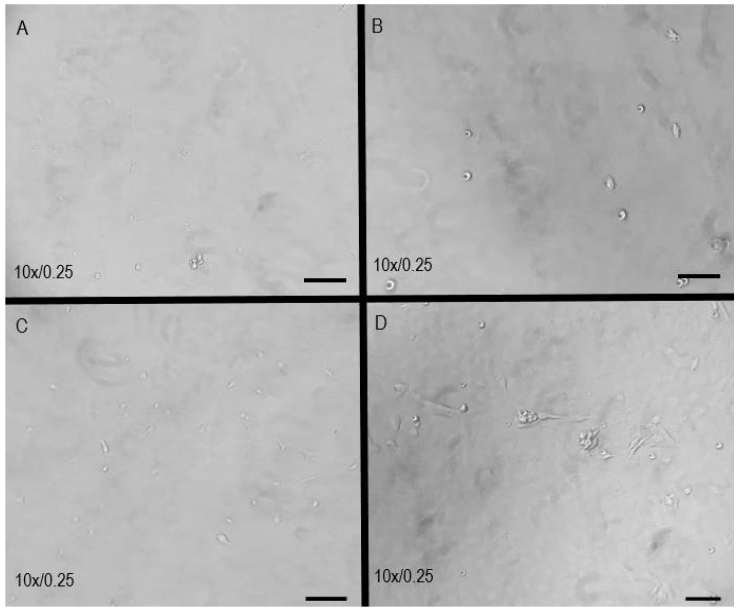

Notes: Phase contrast, bar = 500 micron, amplification x250.

Figure 8 Microchannel images taken of model of PDMS channels in 35 mm culture dishes by conventional brightfield microscope. Skeletal muscle myocytes from mouse neonates seeded in model of PDMS channels in 35 mm culture dishes, (a) day 1 first prototype (b) day 4 first prototype (c) day 1 second prototype (d) day 4 second prototype (e) day 1 third prototype (f) day 4 third prototype

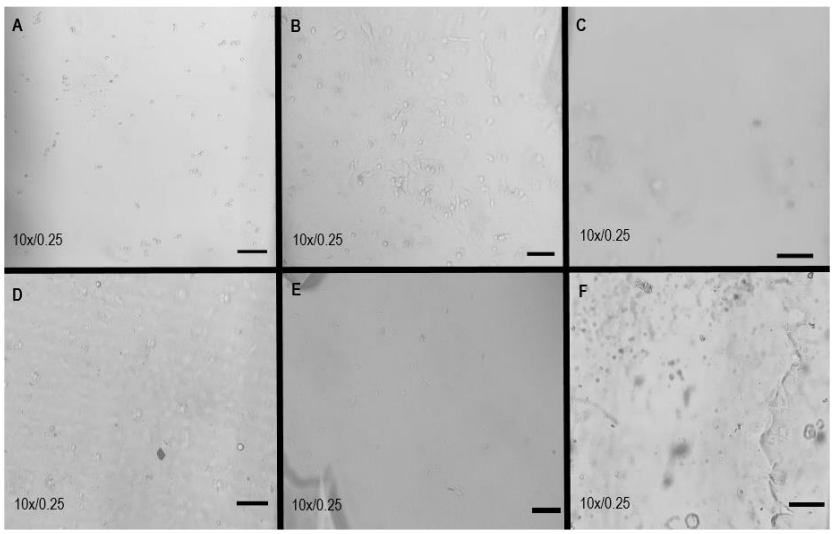

Note: Phase contrast, scale bar = 500 micron, amplification x250.

In Figures 8(a), 8(c) and 8(e) a low cell proliferation was observed. On the fourth day Figures 8(b), 8(d) and 8(f) differentiated and anchored cells are observed, where a greater amount of cell population is observed in the first and third prototype.

Figure 9 Microchannel images taken of the model of PDMS OoC on slides by conventional brightfield microscope. Skeletal muscle myocytes from mouse neonates seeded in PDMS OoC model microchannels on slides, (a) day 1 of the first prototype (b) day 4 of the first prototype (c) day 1 of the second prototype (d) day 4 of the second prototype (e) day 1 to the third prototype (f) day 4 of the third prototype

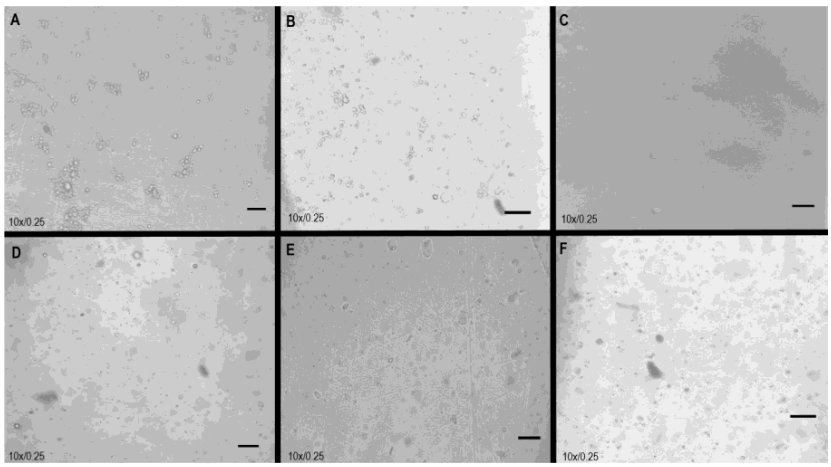

Note: Phase contrast, Scale Bar = 500 micron, Amplification x250.

In Figures 9(a), 9(c) and 9(e) the first prototype is the one with the highest proliferation compared to the others. The third prototype had less cell proliferation. On the fourth day Figures 9(b), 9(d) and 9(f) it is observed that the first prototype had most of cells conglomerated. In the third prototype, there was less cell density from day 1 to day 4.

3.3 High resolution images obtention

Microchannels are made of PDMS, a polymer highly used in biomedical applications for rapid prototyping, but mechanical deformation often occurs in this polymer. The images obtained by the SEM showed an adequate dispersion of the components, but there were irregularities in the microchannels, as well as accumulation of burrs and deformation in the corners as can be seen, these were caused for the mechanical manipulation at the moment of detaching the microchannels from manufacturing mould, see Figure 10.

3.4 Alignment analysis by ImageJ

The angles were measured using ImageJ program, to observe the angle reading procedure. The images in Figures 7, 8 and 9 were sectioned by horizontal lines and the angles were measured respect to the horizontal. Twelve measurements of the angle of the cells were made in each image, to obtain the statistical results with Minitab.

Figure 10 Microchannel structure

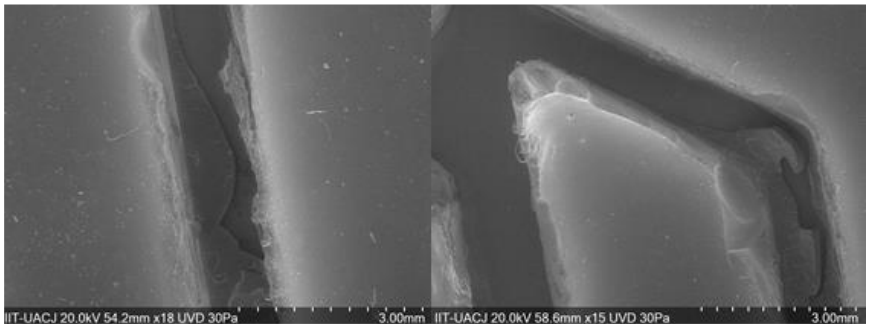

Note: Images taken by SEM (Hitachi, Mod. SU5000) (3.00 mm)

3.5 Statistical analysis of alignment degree using Minitab

A statistical study was carried out with representative samples of a population, 12 angle measurements of the prototypes were taken every 24 hours, the data were only taken from the first day of seeding and the fourth day to see the contrast of population growth and analyse their distribution, the data were analysed with the help of the Minitab program. Statistical tools were used to compare alignment on a culture dish and with microchannel-guided alignment of two types of prototype models by PDMS. The data of the mean were very similar since it circulates at 45°. The difference is the number of cells aligned. On the first day, clustered cells were found aligned, but not anchored. While on the fourth day many anchored cells were observed, and myoblast began to fusion. Various investigations have attempted to search for cell alignment by means of hydrogel rails or by soft polymeric films. The alignment models for hydrogel rails found that a notable factor is the width of the rails, because if the area is large only the cells that are close to the perimeter edges are the ones that will be aligned, while the cells that are further from the perimeter will have a disorganised cell growth (Aubin et al., 2010). Regarding the alignment models for soft polymeric films such as liquid crystal films, they have been found to aid cell alignment due to their homogeneous flat surface, demonstrating that the order of the liquid crystal can be used to manipulate cell growth by transferring information contained within from polymer at molecular level to cell culture (Martella et al., 2019). To observe the trend of angles measured in the culture dish and in the three prototypes of two types of models, the statistical tool, the histogram, was used to obtain the type of angle distribution that the myocytes follow during growth phase. In Figure 11, a greater trend is observed at the angle 41°–47°, the normal distribution lines are trying to approach 40°, however there is a dispersion due to the mean difference.

In Figure 11(a) the alignment angles show a random distribution. Day 1 is symmetrical, it is more convex, there is less variation in the degrees of cell alignment, whereas as the days progress, the standard deviation increases, so there is a greater dispersion of cell growth. In Figure 11(b) the first prototype from days 1 to 4 has a smaller standard deviation so the curve becomes more convex. The second prototype has a greater mean variation while at the beginning it went to the 50° angle on the fourth day it leans to the 37° angle and the dispersion of the data is similar. The third prototype has less angle dispersion, making it the most cell aligned prototype. In Figure 11(c) the first

prototype has a wide variability of the cell alignment angles, but on the fourth day there is a cell alignment around 35°, its standard deviation was reduced to 50%. The second prototype behaves ideally, since on the first day it has greater dispersion of angles and on the fourth day the cells are already aligning. The third prototype does not behave normally, since the first day has greater alignment than on the fourth day, this was because of the irregularities in the microchannels.

Figure 11 Normal distribution in culture plates and prototypes of OoC. Variables A, B, C of Figures 8(b) and 8(c) refers to the first, second and third prototype of each model, (a) normal distribution in culture plates (b) normal distribution in prototype of the PDMS channel model in 35 mm culture plates (c) normal distribution in prototype of the OoC model of PDMS on slides (see online version for colours)

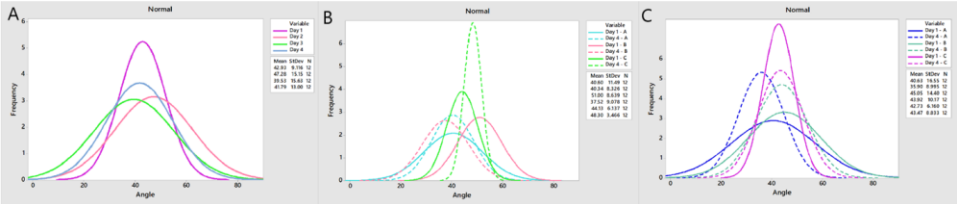

3.6 Nuclear staining with Hoechst

Hoechst nuclear staining is optimal for living cells as it passes through the cell membrane. Hoechst is a compound derived from bis-benzimidazole that binds to the minor groove of DNA. The Hoechst is yellow in its dissolved form, but once it receives UV light through the ZEISS microscope a light is emitted. In the results of the nuclear staining with Hoechst in culture dishes in Figure 12(a) muscle cells can be seen with four days of culture observed in bright field, which in Figure 12(b) have the cell nucleus marked by the Hoechst substance to study cell viability. The cells were anchored to the culture dish, although there are still some suspended cells in the medium because of their round shape, The cell nucleus marked with light confirms that the cells seen in the bright field are alive and agree with the cell nucleus stained with UV light, the image was superimposed on Figure 12(a) and 12(b), see Figure 12(c), it was verified that the cells of Figure 12(b) grow gradually showing good viability, since the largest cell population is stained.

Figure 13 shows muscle cells anchored in a prototype of the model of PDMS channels in 35 mm culture dishes, these images were obtained by the Zeiss inverted fluorescence microscope. Most of the cells were anchored in the corners of the microchannels, due to irregularities in the surface of the prototype. In Figure 13(a) the cell nucleus is marked by the Hoechst substance to study cell viability. In Figure 13(b) Muscle cells can be seen with four days of culture on PDMS channels in 35 mm culture dishes model observed in bright field. Nucleus stained with UV light exposed in Figures 13(a) and 13(b) in bright field were overlaid to compare cell viability, see Figure 13(c).

Figure 12 Nuclear staining by Hoechst in culture plates, (a) image taken by conventional clear field microscope (b) image taken by UV microscope to see nuclear staining with Hoechst (c) overlay (see online version for colours)

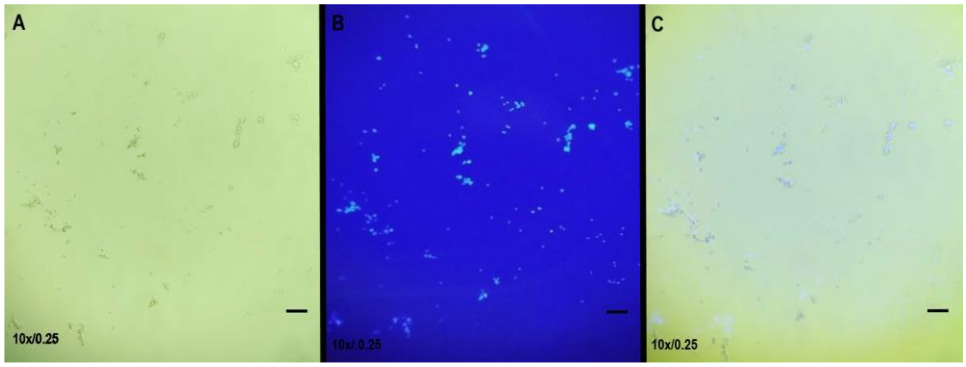

Figure 13 Nuclear staining by Hoechst in prototype of the PDMS channels in 35 mm culture dishes model, (a) image taken by UV microscope to see nuclear staining with Hoechst (b) image taken by conventional clear field microscope (c) overlay (see online version for colours)

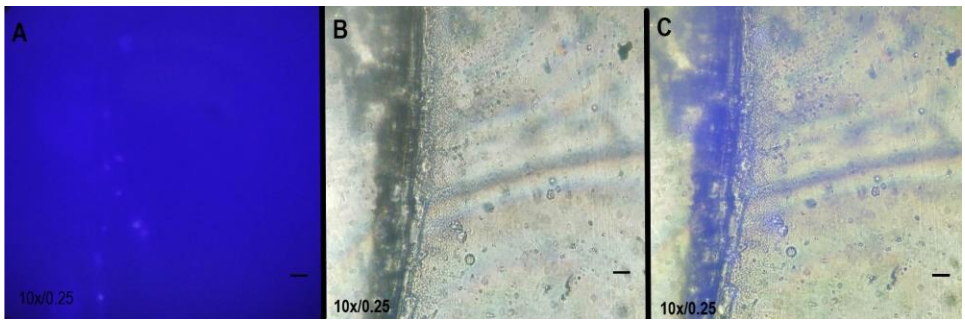

Figure 14 Nuclear staining by Hoechst in prototype of the OoC model of PDMS on slides, (a) Image taken by UV microscope to see nuclear staining with Hoechst (b) image taken by conventional clear field microscope (C) overlay (see online version for colours)

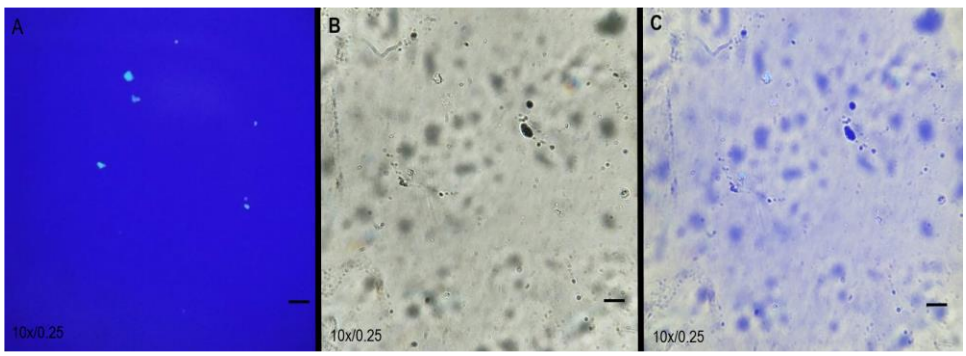

In Figure 14, the nucleus stained by the Hoechst compound are seen in Figure 13(a), in Figure 13(b) a major cell population can be seen in bright field and in Figure 13(c) they are superimposed to identify if they are viable. This lies in the preparation of the prototype; therefore, this type of prototype helps the cells to have a greater growth.

4 Conclusions

Based on the methodology and the results, it is concluded that the protocols for the extraction of skeletal muscle tissue from mouse neonates were successfully applied to achieve a good cell model. Likewise, muscle cells were seeded in culture dishes and in microchannels to observe their growth, development, and alignment. Cell viability was analysed by nuclear staining with Hoechst, it was observed that cell viability was affected by the microchannel depth factor, in the OoC of prototypes with less depth in their microchannels, cell proliferation was low than the microchannels with major depth. It had lower cell proliferation because cell growth was decentralised, turning towards the periphery of the microchannels. Microchannels that were deeper had better viability than those that were shallower. The microchannels of the PDMS channels in 35 mm culture dishes model were the best due to their depth, but the third of the three prototypes were the one with fewer irregularities in the microchannels and a greater depth, which resulted in good cell viability. In addition, the alignment of the cells in the microchannels and the morphology of the cell culture were analysed by light microscopy and the ImageJ program, the results of the angles measured by the ImageJ program were the basis for the statistical analysis of the degree of cell alignment in the microchannels with Minitab, which showed the difference regarding cell alignment in culture dishes and in the two prototype models. In the culture dishes the dispersion of the angles was lower in the first day than in the fourth day. Regarding the PDMS channels in 35 mm culture dishes model, the third was the one that had a better alignment due to the depth of its channels and that there was no obstruction or deformation by mechanical manipulation. In the prototypes of the OoC model of PDMS on slides, the first was the one that had a better alignment of almost 50% reduction in dispersion from day 1 to day 4, because greater the area, greater the proliferation, they also had a greater depth. With the help of the SEM, the morphology of the microchannels of the prototypes could determine that the prototypes had damage in the formation of the microchannels, the material was well-formed, but it had a lot of burrs and in some parts of the microchannels the passage was closed, causing the behaviour of the cells and their growth to be affected, in some areas there was some detachment of the PDMS by mechanical manipulation at the time of detaching the microchannels from the manufacturing mould. Based on the above, it has been demonstrated that the prototype of in-vitro maintenance system type OoC for skeletal muscle of mouse neonates is functional and aids cell alignment. This could be corroborated because cell proliferation was demonstrated proper and aligned according to the time in the microchannels of the prototypes, this was affected by the depth of the microchannels. It is concluded that the two OoC prototype models delimit and help cell alignment, but because the surface of the microchannels was not homogeneous or completely flat, adding to this the depth factor, these conditions caused the cell seeding to overflow and affect cell proliferation. Furthermore, these irregularities caused the cells to anchor in areas where they found optimal anchorage areas. As a recommendation, improve the technique that was performed of emptying by guideline delimitation because

the cell culture was seen affected by the loss of the morphology of the prototype in mechanical manipulation disfavouring cell proliferation. In addition, improve the use of MEMS technology micro-fabrication techniques ensuring the dimensional unification of the channels and a homogeneous distribution of the material.

References

AFM and ASEM (2003) 'El Músculo', *ASEM (Federación española de Enfermedades Neuromusculares)*, Technical Report AFM 06/03 and ASEM 02/2005, ASEM (Federación española de Enfermedades Neuromusculares), Barcelona, España [online] http://www.asemgalicia.com/wp-content/uploads/El-musculo-esqueletico.pdf (accessed 15 June 2020).

Aubin, H. et al. (2010) 'Directed 3D cell alignment and elongation in microengineered hydrogels', *Biomaterials*, Vol. 31, No. 27, pp.6941–6951, Elsevier Ltd., DOI: 10.1016/j.biomaterials.2010.05.056.

Caballero, D. et al. (2017) 'Organ-on-chip models of cancer metastasis for future personalized medicine: from chip to the patient', *Biomaterials*, Vol. 149, pp.98–115, Elsevier Ltd., DOI: 10.1016/j.biomaterials.2017.10.005.

Crowley, L.C., Marfell, B.J. and Waterhouse, N.J. (2016) 'Analyzing cell death by nuclear staining with Hoechst 33342', *Cold Spring Harbor Protocols*, DOI: 10.1101/pdb.prot087205.

Halldorsson, S. et al. (2015) 'Advantages and challenges of microfluidic cell culture in polydimethylsiloxane devices', *Biosensors and Bioelectronics*, Vol. 63, pp.218–231, Elsevier, DOI: 10.1016/j.bios.2014.07.029.

Jena, B.P. et al. (2019) 'Human skeletal muscle cell atlas: unraveling cellular secrets utilizing 'muscle-on-a-chip', differential expansion microscopy, mass spectrometry, nanothermometry and machine learning', *Micron*., November, Vol. 117, pp.55–59, Elsevier, DOI: 10.1016/j.micron.2018.11.002.

Martella, D. et al. (2019) 'Liquid crystal-induced myoblast alignment', *Advanced Healthcare Materials*, Vol. 8, No. 3, pp.1–10, DOI: 10.1002/adhm.201801489.

Materne, E.M. et al. (2015) 'A multi-organ chip co-culture of neurospheres and liver equivalents for long-term substance testing', *Journal of Biotechnology*, Vol. 205, pp.36–46, Elsevier B.V., DOI: 10.1016/j.jbiotec.2015.02.002.

Sakolish, C.M. et al. (2016) 'Modeling barrier tissues in vitro: methods, achievements, and challenges', *EBioMedicine*, Vol. 5, pp.30–39, DOI: 10.1016/j.ebiom.2016.02.023.

Sun, W. et al. (2016) 'Organs-on-chips and its applications', *Chinese Journal of Analytical Chemistry*, Vol. 44, No. 4, pp.533–541, Changchun Institute of Applied Chemistry, Chinese Academy of Sciences, DOI: 10.1016/S1872-2040(16)60920-9.

Wilmer, M.J. et al. (2016) 'Kidney-on-a-chip technology for drug-induced nephrotoxicity screening', *Trends in Biotechnology*, Vol. 34, No. 2, pp.156–170, Elsevier Ltd., DOI: 10.1016/j.tibtech.2015.11.001.

Zuñiga Aguilar, E.S. (2014) *Crecimiento volumétrico de células de músculo esquelético y motoneuronas de ratón en fibras electrohiladas de PLA y PLA-PPy*, Unpublished PhD thesis, Universidad Autónoma Metropolitana Unidad Iztapalapa, Mexico City, Mexico.